the plant journal

SEB SOCIETY FOR EXPERIMENTAL BIOLOGY

The Plant Journal (2020) doi: 10.1111/tpj.14914

WRKY42 transcription factor positively regulates leaf senescence through modulating SA and ROS synthesis in *Arabidopsis thaliana*

Fangfang Niu[1], Xing Cui[1], Peiyu Zhao[1], Mengting Sun[1], Bo Yang[1,*], Michael K. Deyholos[2], Ye Li[1], Xinjie Zhao[1] and Yuan-Qing Jiang[1,*]

[1]*State Key Laboratory of Crop Stress Biology for Arid Areas, College of Life Sciences, Northwest A & F University, Yangling, Shaanxi 712100, China, and*

[2]*Department of Biology, University of British Columbia, Okanagan Campus, Kelowna, BC V1V 1V7, Canada*

Received 15 November 2019; revised 18 June 2020; accepted 25 June 2020.
*For correspondence (e-mails jiangyq@nwafu.edu.cn; yangwl@nwafu.edu).

SUMMARY

Leaf senescence represents the final stage of leaf growth and development, and its onset and progression are strictly regulated; however, the underlying regulatory mechanisms remain largely unknown. In this study we found that *WRKY42* was highly induced during leaf senescence. Loss-of-function *wrky42* mutants showed delayed leaf senescence whereas the overexpression of *WRKY42* accelerated senescence. Transcriptome analysis revealed 2721 differentially expressed genes between wild-type and *WRKY42*-overexpressing plants, including genes involved in salicylic acid (SA) and reactive oxygen species (ROS) synthesis as well as several senescence-associated genes (SAGs). Moreover, WRKY42 activated the transcription of *isochorismate synthase 1* (*ICS1*), *respiratory burst oxidase homolog F* (*RbohF*) and a few SAG genes. Consistently, the expression of these genes was reduced in *wrky42* mutants but was markedly increased in transgenic Arabidopsis overexpressing *WRKY42*. Both *in vitro* electrophoretic mobility shift assays (EMSAs) and *in vivo* chromatin immunoprecipitation and dual luciferase assays demonstrated that WRKY42 directly bound to the promoters of *ICS1* and *RbohF*, as well as a few *SAG*s, to activate their expression. Genetic analysis further showed that mutations of *ICS1* and *RbohF* suppressed the early senescence phenotype evoked by *WRKY42* overexpression. Thus, we have identified WRKY42 as a novel transcription factor positively regulating leaf senescence by directly activating the transcription of *ICS1*, *RbohF* and *SAG*s, without any seed yield penalty.

Keywords: Arabidopsis, leaf senescence, reactive oxygen species, salicylic acid, *WRKY42*.

INTRODUCTION

Leaf senescence, an important developmental process that is critical for plant fitness, orderly disassembles macromolecules to remobilize nutrients to growing leaves, fruits and seeds (Gan and Amasino, 1997; Lim *et al.*, 2007; Schippers *et al.*, 2015). It is regulated by developmental programs integrated with other internal and external environmental signals (Lim *et al.*, 2007; Schippers *et al.*, 2015). The internal signals include reproductive development, reactive oxygen species (ROS) and various phytohormones. The hormones abscisic acid (ABA), ethylene (ET), jasmonic acid (JA) and salicylic acid (SA) accelerate senescence, whereas cytokinin and auxin delay senescence (Grbić and Bleecker, 1995; Gan and Amasino, 1997; Morris *et al.*, 2000; He *et al.*, 2002; Lim *et al.*, 2007; Mhamdi and Van Breusegem, 2018). Environmental cues for the onset and progression of senescence include darkness, nutrient limitation, drought, and oxidative and osmotic stresses (Guo and Gan, 2005; Lim *et al.*, 2007; Woo *et al.*, 2016).

Leaf senescence is also a form of programmed cell death (PCD) that is coordinated by massive gene regulatory networks, and involving a specific set of senescence-associated genes (SAGs) (Gepstein *et al.*, 2003; Lim *et al.*, 2007). The proteins encoded by SAGs are diverse and are implicated in macromolecule degradation, nutrient remobilization, the transport and detoxification of metabolites as well as stress tolerance (Gepstein *et al.*, 2003; Lim *et al.*, 2007). It has been documented that the expression of many SAGs is also affected by environmental stressors and hormones (Lim *et al.*, 2007), suggesting extensive crosstalk between senescence and stress responses. Precocious leaf senescence usually causes a dramatic reduction in crop yields;

therefore it is challenging to breed a crop with a shortened life cycle without any loss in yield.

Salicylic acid (SA) regulates innate immunity and various developmental processes in plants (Dempsey *et al.*, 2011). SA concentration is controlled by its biosynthesis and catabolism (Zhang and Li, 2019). SA is mainly synthesized through the isochorismate pathway in the chloroplasts of plants, with ICS1 (isochorismate synthase 1, also termed SA induction-deficient 2, SID2) being a critical enzyme (Wildermuth *et al.*, 2001). In Arabidopsis, ICS1 appears to be responsible for 90% of SA production induced by pathogens or UV light, whereas ICS2 contributes to the basal SA synthesis (Garcion *et al.*, 2008). More recently, two independent reports have elucidated the last two steps in the isochorismate-derived SA biosynthetic pathway, in which the cytosolic enzyme avrPphB susceptible 3 (PBS3) catalyzes the conversion of isochorismate into an unstable intermediate, isochorismate isochorismoyl-glutamate (ISC-9-Glu), which then spontaneously forms SA, although EPS1, a BAHD acyltransferase-family protein, accelerates this process (Rekhter *et al.*, 2019; Torrens-Spence *et al.*, 2019).

A crucial role for SA in leaf senescence has been established based on several observations. First, SA concentration increases in an age-related manner during leaf development, altering the expression of a number of *SAG*s (Morris *et al.*, 2000; Breeze *et al.*, 2011). Second, transgenic plants overexpressing the *NahG* salicylate hydroxylase have considerably reduced SA concentrations, and exhibit a delayed leaf senescence phenotype in an age-dependent manner (Morris *et al.*, 2000; Lim *et al.*, 2007). Third, mutants defective in SA signaling in Arabidopsis, such as *nonexpressor of pathogenesis-related genes 1* (*npr1*) and *phytoalexin deficient 4 (pad4)*, exhibit dramatically reduced *SAG* expression and delayed leaf senescence (Morris *et al.*, 2000; Lim *et al.*, 2007).

As one of the earliest cellular responses during senescence, ROS production has been reported to play a crucial role in regulating this process (Leshem, 1988; Khanna-Chopra, 2012; Woo *et al.*, 2013). The concentration of hydrogen peroxide (H_2O_2), a relatively stable ROS, increases during the developmental transition to bolting (Ye *et al.*, 2000; Zimmermann *et al.*, 2006). High concentrations of ROS cause oxidation, and damage proteins, lipids and other macromolecules (Apel and Hirt, 2004), which is typical of the degradation of cellular components observed during senescence (Lim *et al.*, 2007). At lower concentrations, ROS function as signaling molecules to regulate many biological processes (Mittler, 2017). In plants, a small family of respiratory burst oxidase homologs (Rbohs; orthologs of mammalian NADPH oxidases), are localized at the plasma membrane and generate ROS in the apoplast (Torres and Dangl, 2005). Among these, RbohD and RbohF also function in ROS-dependent ABA signaling (Kwak *et al.*, 2003). RbohD also plays an important role in cell death control, and systemic signaling upon challenge by biotic and abiotic stresses, and RbohF may act redundantly with RbohD in some pathways (Torres *et al.*, 2002; Torres *et al.*, 2005; Miller *et al.*, 2009). It has been reported that there is crosstalk between ROS and SA, in that H_2O_2 stimulates SA biosynthesis in *Nicotiana tabacum* (tobacco) and SA influences H_2O_2 production and H_2O_2-metabolizing enzymes (Leon *et al.*, 1995; Rao *et al.*, 1997). A more recent study indicates that SA accumulation is not induced by H_2O_2 in Arabidopsis, however (Hieno *et al.*, 2019). Whether SA and H_2O_2 production is controlled by a single transcription factor (TF) remains unknown.

Many TFs are differentially expressed during leaf senescence in Arabidopsis and other plants, including several members of the WRKY family (Guo *et al.*, 2004; Balazadeh *et al.*, 2008; Breeze *et al.*, 2011). Furthermore, SA treatment affects the expression of more than 70% of the *WRKY* gene family members in Arabidopsis, suggesting an important role for WRKY-mediated transcriptional control in leaf senescence (Dong *et al.*, 2003). So far, the functions and regulatory mechanisms of a few WRKY TFs in leaf senescence have been characterized in Arabidopsis (Robatzek and Somssich, 2001; Miao *et al.*, 2004; Zhou *et al.*, 2011; Besseau *et al.*, 2012; Jiang *et al.*, 2014; Chen *et al.*, 2017). These WRKY TFs do not exert their functions in leaf senescence through SA and/or ROS, however, except for the two most recent reports, in which AtWRKY75 was shown to positively regulate leaf senescence through increasing SA production by inducing *SID2* transcription (Guo *et al.*, 2017; Zhang *et al.*, 2017) and repressing H_2O_2 scavenging by suppressing *catalase 2* (*CAT2*) transcription (Guo *et al.*, 2017). However, whether any TFs positively regulate ROS- and SA-synthesis-related gene expression remains unknown. Moreover, the roles that many other WRKY TFs play in leaf senescence remain largely unknown. In a previous transcriptome sequencing (RNA-seq) study, we found that the expression of *WRKY42* was highly induced during the progression of leaf senescence, and also found that the *ICS1* promoter was regulated by WRKY42 through a yeast one-hybrid screening. We thus hypothesized that WRKY42 may play an important role in leaf senescence, except the reported role in phosphate homeostasis (Su *et al.*, 2015). In the present study, we show that WRKY42 is a novel senescence TF (sen-TF) that positively regulates leaf senescence by modulating SA and H_2O_2 production in Arabidopsis, without seed yield penalty.

RESULTS

WRKY42 is a senescence-associated gene

WRKY42 encodes a transcription factor that harbors a single DNA-binding WRKY domain and is localized exclusively to the nucleus (Figure S1a,b). A yeast two-hybrid

assay indicated that WRKY42 interacted with itself, which was further confirmed through a bimolecular fluorescence complementation (BiFC) assay (Figure S1c,d). To study the role of WRKY42 in leaf senescence, we first used qRT-PCR to measure transcript levels of *WRKY42* during the progression of leaf senescence. We assayed Arabidopsis leaves at four developmental stages, namely: young (YL), mature (ML), early senescence (ES) and late senescence (LS) (Figure 1a). The results showed that the *WRKY42* transcript level was significantly increased in ES, compared with the earlier stages, and then increased further in LS (Figure 1b). Moreover, *WRKY42* was expressed in a spatial gradient along the long axis (tip, middle and base) of late senescent leaves (Figure 1b). Furthermore, a histochemical staining of 35-day-old transgenic Arabidopsis expressing β-glucuronidase (GUS) driven by the 2-kb *WRKY42* upstream genomic region displayed higher GUS activity in yellowing and senescing leaves than that in young and green leaves (Figure 1c), supporting the finding that *WRKY42* transcription is induced during leaf aging and is a senescence-associated gene.

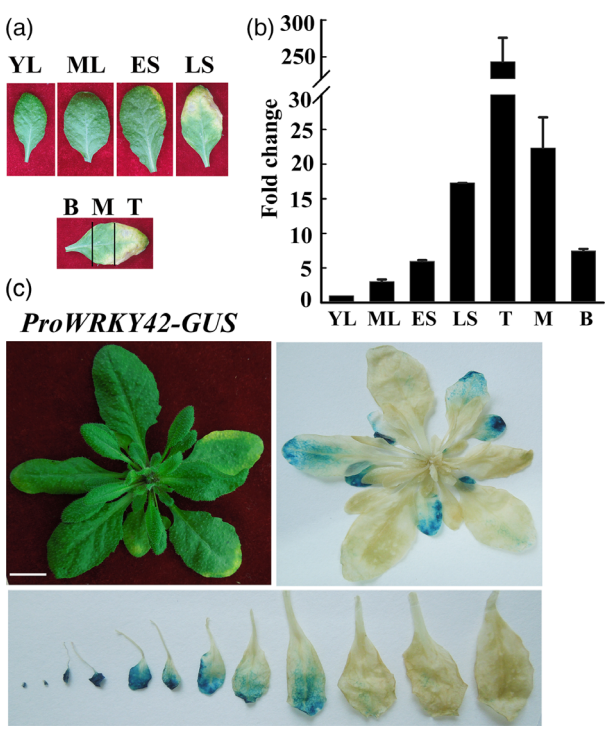

Figure 1. Expression analysis of *WRKY42* during leaf senescence in Arabidopsis.
(a) Wild-type (wt) leaves at different developmental stages. YL, young leaf at 21 days old; ML, mature leaf at 28 days old; ES, early senescent leaf at 35 days old; LS, late senescent leaf at 42 days old. B, M and T indicate the base, middle and tip section of a late senescent leaf at 42 days old, respectively.
(b) qRT-PCR analysis of *WRKY42* transcript levels in leaves at different developmental stages. Data are means ± standard error (SE) of three independent biological replicates. *UBQ10* and *UBC21* were used as internal controls. (c) GUS staining of rosette leaves of 35-day-old *ProWRKY42-GUS* transgenic plant. The seedling before stained was shown beside. Bar, 1 cm.

Overexpression of *WRKY42* promotes age-dependent leaf senescence

To investigate the function of *WRKY42* in senescence further, we produced two *WRKY42*-overexpressing transgenic plants (*WRKY42-OE29* and *-OE13*) under the control of the cauliflower mosaic virus (CaMV) *35S* promoter. *GFP*-overexpressing transgenic plants were generated as controls besides the wild-type (wt) controls. The accumulation of *WRKY42* transcripts and proteins in these two transgenic lines of *OE29* and *OE13* was quantified by quantitative reverse transcriptase polymerase chain reaction (qRT-PCR; Figure 2a) and immunoblotting (Figure 2b), respectively. The phenotypes of transgenic plants were examined at several different developmental stages. *WRKY42-OE* plants displayed obviously precocious leaf senescence symptoms compared with wild-type and *GFP* lines at 35 days old (Figure 2c). The *WRKY42-OE* plants started to exhibit leaf yellowing symptoms at 30 days (Figures S2 and S3a,c) and showed serious leaf cell death at 42 days (Figure S3a), whereas the rosette leaves of wt and *GFP* plants began to turn yellow at 35 days (Figure S3a). Changes in the chlorophyll abundance (Figure 2e) and ion leakage (Figure 2f) of rosette leaves were consistent with precocious leaf senescence in the overexpression lines, which resulted in a lower chlorophyll content and higher ion leakage (represented by relative conductivity) (Figure 2e–f). We also monitored the expression of a senescence marker gene *SAG12* (Noh and Amasino, 1999) and found that the *SAG12* expression level was significantly higher in *WRKY42*-OE plants than in controls, whereas its level was markedly lower in the two *wrky42* mutants than in the wt (Figure S4). In addition, an earlier flowering phenotype was observed in *WRKY42-OE* lines (Figure S3e,f), indicating that WRKY42 accelerates the reproductive transition along with leaf aging and shortens plant lifespan. Interestingly, no significant difference in the seed mass per plant was observed among the *wrky42* mutants, *WRKY42-OE* plants and controls (Figure S5), showing that the overexpression of *WRKY42* can shorten the life cycle of Arabidopsis without affecting its yield.

Leaf aging is also accompanied by increasing ROS levels, and H_2O_2 (one type of ROS) could act as a signal for triggering cell death during senescence (Van Breusegem and Dat, 2006). We therefore tested whether WRKY42-induced leaf senescence is dependent on H_2O_2 accumulation. H_2O_2 production was visualized using 3,3′-diaminobenzidine (DAB) staining, which produced a denser blue color in *WRKY42-OE* lines than in wt and *GFP* plants (Figure 2d). The content of H_2O_2 in the rosette leaves of *WRKY42-OE* plants was further quantified, and it was higher than in the wt or *GFP* control plants (Figure 2g). These results show

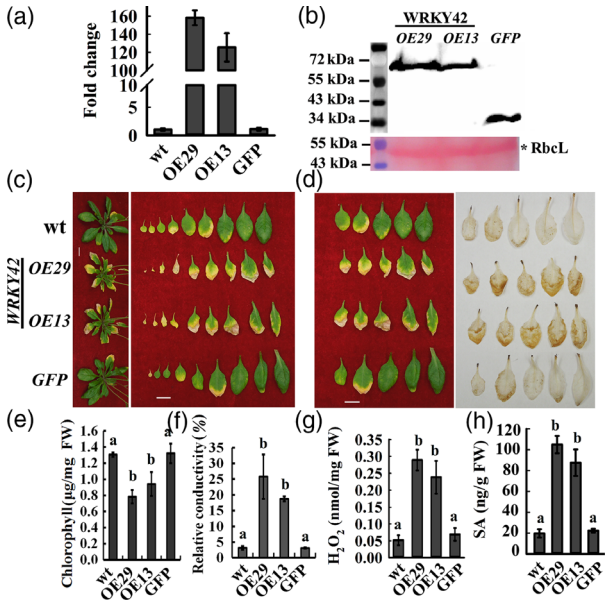

Figure 2. Overexpression of *WRKY42* promotes age-dependent leaf senescence.
(a) qRT-PCR analysis of *WRKY42* transcript levels in wt, two overexpression lines OE29, OE13 and *GFP* transgenic line. Data are means ± SE of three independent biological replicates. *UBQ10* and *UBC21* were used as internal controls. The expression level of *WRKY42* in wt was set as 1. (b) Western blot analysis of WRKY42 expression level in overexpression lines and *GFP* transgenic plants. Anti-HA antibody was used to detect the WRKY42-HA or GF-HA protein. Ponceau S staining of the large subunit of Rubisco (RbcL) as a sample loading control was shown at the bottom. (c) Leaf senescence phenotype of 35-day-old wt, *WRKY42-OE29*, *OE13* and *GFP* transgenic plants. The rosette leaves (true leaves) 1st −9th were placed for comparing the senescent phenotype. Scale bar, 1 cm. (d) DAB staining of the 5th −9th rosette leaves (true leaves, from the same set of plants as shown in c) of different genotypes. (e–g) Quantification of chlorophyll content (e), relative conductivity (f), H_2O_2 content (g) and SA content (h) of the 5th-8th rosette leaves. Values are means ± SE of three independent biological replicates. Identical and different letters represent non-significant and significant differences (two-way ANOVA, $P < 0.05$).

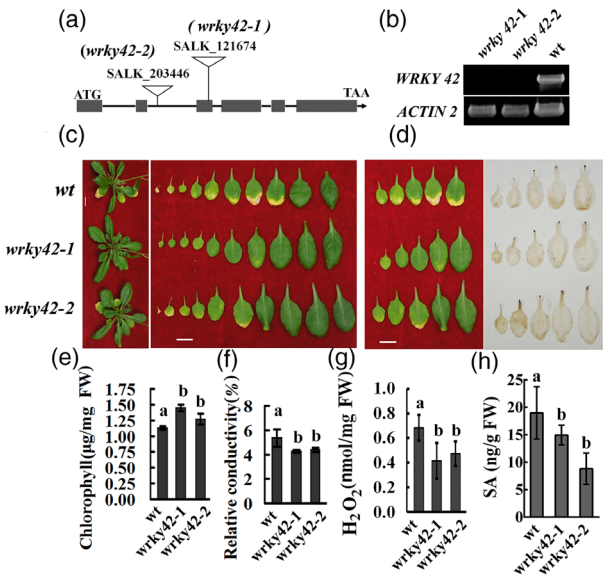

Figure 3. Loss of *WRKY42* function delays age-triggered leaf senescence.
(a) Gene structure of *WRKY42* and location of T-DNA insertions. Rectangles represent exons and lines denote introns. Two SALK mutants were obtained for *WRKY42*. (b) RT-PCR analysis of *WRKY42* expression in two T-DNA insertion lines and wt. *ACTIN2* was amplified as an internal control. (c) Leaf senescence phenotype of 35-day-old wt, *wrky42-1* and *wrky42-2*. The rosette leaves (true leaves) 1st −9th were placed in a row for comparison. Scale bar, 1 cm. (d) DAB staining of the 5th-9th rosette leaves (true leaves, from the same set of plants as shown in c) of wt and two *wrky42* mutant lines. (e–g) Measurements of chlorophyll content (e), relative conductivity (f), H_2O_2 content (g) and SA content (h) in the 5th-8th rosette leaves. Values are means ± SE of four independent biological replicates. Identical and different letters represent non-significant and significant differences (two-way ANOVA, $P < 0.05$).

that constitutive overexpression of *WRKY42* accelerates leaf senescence in an age-dependent manner, which could be associated with increased H_2O_2 accumulation.

Loss of *WRKY42* function delays age-dependent leaf senescence

To further confirm the role of *WRKY42* in age-triggered leaf senescence, two T-DNA insertion mutants, SALK_121674 (*wrky42-1*) and SALK_203446 (*wrky42-2*), were obtained. An RT-PCR assay indicated that these two mutants are knockout alleles, as *WRKY42* transcript was not detectable in either of the two mutant lines (Figure 3a,b). A significantly delayed leaf senescence was observed in both *wrky42* mutants compared with the wt at 35 days (Figure 3c), and also at 42 and 49 days (Figure S3b). The DAB staining, indicating the H_2O_2 level, also supported the delayed leaf senescence symptom (Figure 3d). Consistently, both mutants displayed higher chlorophyll content (Figures 3e and S3d), lower electrolyte leakage (Figure 3f) and less H_2O_2 accumulation than the wt (Figure 3g). Furthermore, the expression level of *SAG12* in the two mutant lines was significantly lower than that in the wt (Figure S4b). These results were therefore consistent and complementary to precocious senescence in *WRKY42-OE* lines, indicating that WRKY42 functions as a positive regulator in age-dependent leaf senescence.

Transcriptome profiling reveals differentially expressed genes regulated by WRKY42

Next, to explore how WRKY42 regulates leaf senescence, we conducted genome-wide mRNA expression analysis of *WRKY42-OE29* and wt plants at 30 days of age using RNA sequencing (RNA-seq). We identified 2721 differentially expressed genes (DEGs) between *WRKY42-OE29* and the wt ($|\log_2 FC| \geq 1$ and $P < 0.05$) (Figure 4a). Among the DEGs, 1498 genes were upregulated and 1223 genes were downregulated in the *WRKY42-OE29* line, compared with wt (Figure 4a). Gene ontology (GO) enrichment analysis of these DEGs revealed that a wide array of functional

biological processes, including responses to oxygen-containing compounds, defense response, SA biosynthesis and signaling, JA signaling, PCD, ROS metabolic process and aging (Figures 4b and S6).

Among the DEGs, we identified several distinct groups of genes, some of which have been reported to positively regulate leaf senescence (Lim *et al.*, 2007; Li *et al.*, 2012). The first group is the SAG group, including *SAG13*, *SAG21*, *SAG24*, *SAG101*, *SAG103*, *SAG201* and *YLS9/NHL10* (*yellow leaf-specific 9/NDR1/HIN1-like 10*) (Figure 4c). The second group contains genes implicated in SA biosynthesis and signaling, including *ICS1*, *PBS3*, *enhanced disease susceptibility 1* (*EDS 1*), *EDS5*, *pathogenesis-related 1* (*PR1*), *PR5*, *NPR3*, *SIRK*, *CBP60G* and *SARD1*. The third group comprises genes involved in PCD, which are *metacaspase 1* (*MC*), *MC6*, *MC8*, *CEP1* and *CYP76C2*. The fourth group comprises genes implicated in the biosynthesis of ethylene, including *1-aminocyclopropane-1-carboxylate oxidase 2* (*ACO2*), *1-aminocyclopropane-1-carboxylic acid* (*ACC*) *synthase 2* (*ACS 2*) and *ACS6*. The fifth group includes ABA synthesis-related genes: *9-cis-epoxycarotenoid dioxygenases 4* (*NCED 4*), *NCED5* and *aldehyde oxidase 1* (*AAO1*). The sixth group contains JA biosynthesis- and signaling-related genes, and these are *lipoxygenase 1 (LOX 1)*, *LOX5*, *plant defensin 1.3* (*PDF 1.3*), *PDF1.4* and *PDF2.1*. The seventh group contains genes involved in ROS production and signaling, including *RbohF*, *ZAT12* and many H_2O_2-responsive TF-encoding genes of the *WRKY*, *NAC* and *ethylene response factor* (*ERF*) families (Hieno *et al.*, 2019). Interestingly, a few TF genes, including those well-known sen-TF genes, were also upregulated, e.g. *NAC016*, *NAC046*, *NAC055*, *WRKY6*, *WRKY45* and *WRKY75* (Figure 4c). In contrast, a few senescence downregulated genes (SDGs) were found to be repressed in the *WRKY42-OE* line. For example, auxin-responsive genes (*IAA1*, *IAA3*, *IAA5*, *AUX1*, *ARF18*, etc.), *early light-inducible protein 1* (*ELIP1*), *leucoanthocyanidin dioxygenase* (*LDOX*), *RVE3* (encoding an MYB-like TF regulating circadian rhythm) and *SWEET13* (a member of the sucrose efflux transporter family) were downregulated in the *WRKY42-OE29* line (Figure 4c). These results suggest that WRKY42 modulates leaf senescence through a complex regulatory network.

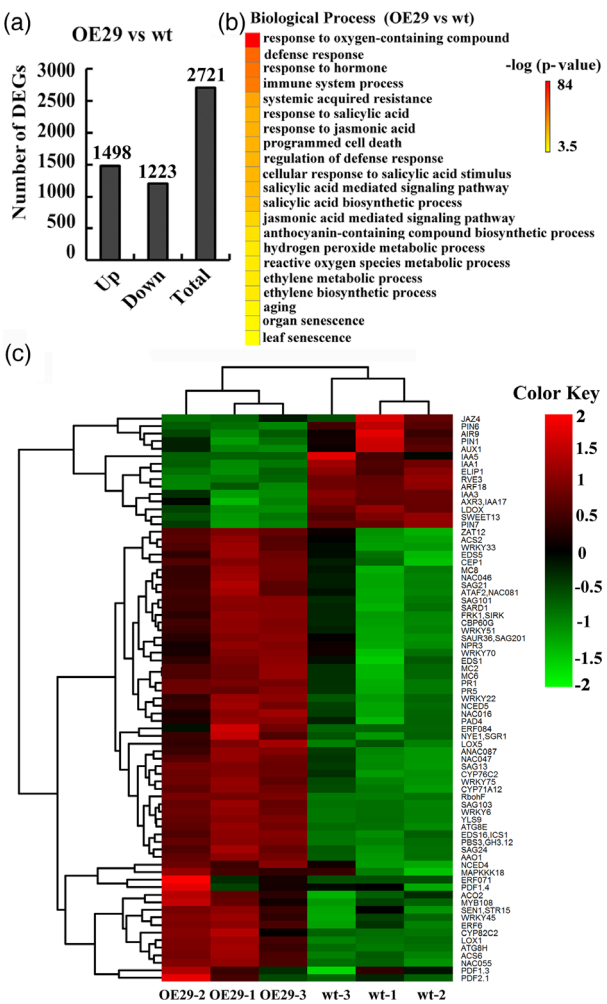

Figure 4. RNA-seq analysis reveals senescence-related genes regulated by WRKY42.

(a) Differentially expressed genes (DEGs) from RNA-seq analysis of the 7th and 8th rosette leaves of 30-day-old *WRKY42-OE29* and wild-type (wt). (b) Functional analysis of the DEGs from RNA-seq through GO analysis, bar represents -log (*P*-value). C, Cluster heatmap analysis of expression of selected DEGs in *WRKY42-OE29* and wt from RNA-seq. The expressions of DEGs are hierarchically clustered on the y-axis, and plant samples are hierarchically clustered on the *x*-axis. The values of DEGs in the six samples are normalized by a scale function. The transcription levels are presented in red and green, which indicate upregulated and downregulated genes by WRKY42, respectively.

Furthermore, to validate the RNA-seq data, 25 upregulated and four downregulated genes were chosen for examination by qRT-PCR in both *WRKY42*-overexpressing and mutant lines, compared with the wt control. Consistent with the RNA-seq analysis, the transcript levels of the 25 upregulated genes were all dramatically increased in the *WRKY42-OE29* line, whereas most of them were significantly decreased in the *wrky42-1* mutant (Figure 5a,b). In contrast, the four downregulated genes (*IAA1*, *PIN1*, *ELIP1* and *LDOX*) also showed an opposite altered expression pattern in the *WRKY42-OE* and mutant plants, compared with the wt (Figure 5b).

The WRKY TFs function by binding directly to the canonical *cis*-element W-box (TTGACC/T) in promoters of target genes (Eulgem *et al.*, 2000). We therefore searched for W-box sequences in the promoters (including the 5′ untranslated region, 5′-UTR) of upregulated genes identified by our RNA-seq analysis, and we found that 1164 (out of 1498) genes have at least one canonical W-box in the 1-kb promoter regions.

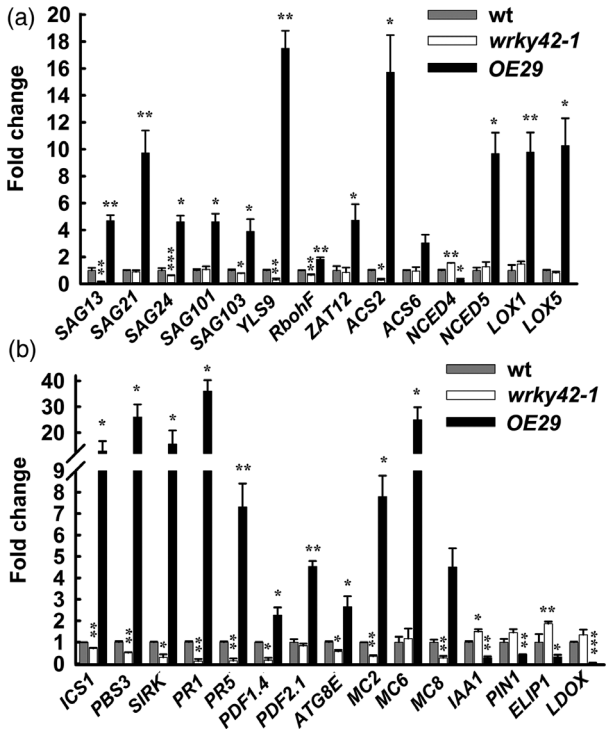

Figure 5. qRT-PCR analysis of transcript levels of senescence-related genes identified through RNA-seq.
(a-b) qRT–PCR was conducted to determine transcript levels of senescence-related genes in 7th and 8th rosette leaves of 30-day-old wt, *wrky42-1* and *WRKY42-OE29* lines. *UBQ10* and *UBC21* were used as internal controls. Value represents the mean ± SE of four biological replicates. Asterisks represent significant differences compared to wt by Student's *t*-test (**P* < 0.05, ***P* < 0.01, ****P* < 0.001).

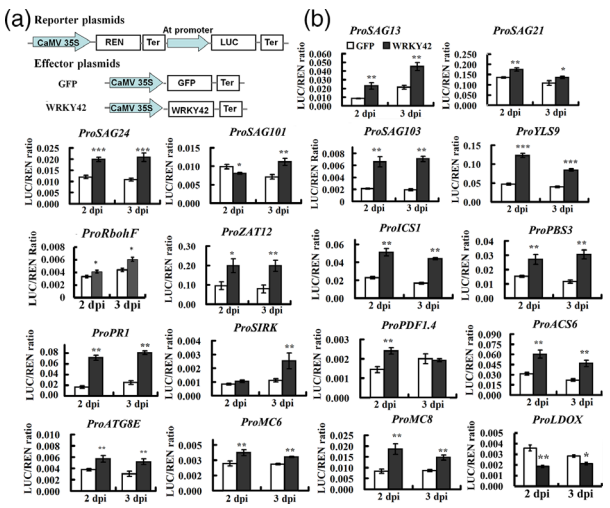

Figure 6. WRKY42 activates the transcription of senescence-related, SA and ROS synthesis, and defense response genes by dual LUC reporter assays.
(a) Schematic diagram of reporter and effector constructs used in the dual luciferase reporter assay. In the reporter plasmids, Renilla (REN) luciferase gene driven by CaMV35S promoter was used as the internal control and, the target gene promoters are fused to the *LUC* (*Firefly Luciferase*). In the effector plasmids, *GFP* (control) and *WRKY42* are driven by CaMV35S promoter. Ter, transcriptional terminator sequence. (b) Dual luciferase reporter assay results. Different combinations of reporter and effecter plasmids were co-infiltrated into leaves of *N. benthamiana*. The ability of WRKY42 to activate the reporter LUC gene was represented by the ratios of LUC to REN. The *35S:REN* served as an internal control. Values indicate the mean ± SE of three biological replicates. Asterisks represent significant differences between WRKY42 and GFP by Student's *t*-test (**P* < 0.05, ***P* < 0.01, ****P* < 0.001).

WRKY42 modulates the transcription of *SAG*s, ROS and SA-synthesis-related genes

To establish a regulatory connection between WRKY42 and the putative downstream targets identified above, we performed a dual luciferase (LUC)-based reporter assay. Different combinations of reporters and effectors, in which *35S:GFP* was used as the control of the effector and *35S:REN* was used an internal control (Figure 6a), were co-expressed, with LUC and REN activities measured sequentially to reflect the transcriptional activity of individual promoters *in vivo* at two different time points. The results showed that co-expression of *35S:WRKY42* with *LUC* driven by 17 promoters significantly increased the LUC/REN ratios compared with the *GFP* effector control at one or two time points (Figure 6b). These promoters included upstream regions from six *SAG*s (*SAG13*, *21*, *24*, *101*, *103* and *YLS9*), four SA-related genes (*ICS1*, *PBS3*, *PR1* and *SIRK*), two ROS-related genes (*RbohF* and *ZAT12*), three PCD and autophagy-related genes (*MC6*, *MC8* and *ATG8E*), *PDF1.4* and *ACS6*, indicating that these 17 genes tested were dramatically activated by WRKY42. As a control, one of the downregulated genes, *LDOX*, was also included in the dual LUC assay. The result showed that the promoter activity of *LDOX* was significantly repressed by WRKY42 (Figure 6b); however, co-expression of *35S:WRKY42* and *LUC* driven by promoters of a few other upregulated genes, such as *ACS2*, *NCED4*, *LOX5* and *PR5*, did not significantly change the LUC/REN ratios (Figure S6), indicating that these genes are not directly regulated by WRKY42. Moreover, *WRKY42* expression significantly repressed the *LUC* expression driven by promoters of *NCED5*, *LOX1*, *PDF1.3*, *PDF2.1* and *MC2* at one or two time points (Figure S7), suggesting that these genes are not likely to be direct targets of WRKY42. In total, among the DEGs examined further, eight genes were dramatically activated by WRKY42 in the dual LUC assay and were also induced in the *WRKY42-OE29* line, whereas they were significantly repressed in the *wrky42-1* mutant line. These include three *SAG*s (*SAG13*, *SAG24* and *SAG103*), three genes involved in SA synthesis and signaling (*ICS1*, *PBS3* and *PR1*), *RbohF* and *YLS9*.

WRKY42 positively regulates the accumulation of SA

Considering the fact that RNA-seq and subsequent pathway and GO analyses uncovered many genes implicated in

the biosynthesis of leaf senescence-promoting hormones, including SA, JA and ABA, we measured the contents of SA, JA and ABA in *WRKY42-OE* and mutant lines, as well as in control lines, in order to further dissect the regulatory roles of WRKY42 in leaf senescence. The free SA contents in the *WRKY42-OE29* and *WRKY42-OE13* leaves were five-fold and fourfold higher than those of the wt and the *GFP* line, respectively (Figure 2h). In contrast, the free SA levels in the two *wrky42* mutants were significantly lower than those of the wt and the *GFP* controls (Figure 3h). Although the levels of JA and ABA were significantly increased in the OE29 line compared with the controls, no significant difference was observed between *wrky42* mutants and control plants (Figure S8a,b). Taken together, these data suggest that, besides inducing ROS accumulation, WRKY42 positively regulates leaf senescence partly by inducing SA accumulation, and that ABA and JA are only likely to exert an indirect or minor role in WRKY42-induced leaf senescence.

WRKY42 directly binds to the promoters of *SAG*s, ROS and SA biosynthesis-related target genes

We further examined the binding of WRKY42 to the promoter regions of the putative target genes *in vitro* and *in vivo*. We identified that there are one or more candidate binding sites, the W-box elements, in the promoters of *SAG13*, *SAG24*, *SAG103*, *ICS1*, *PBS3*, *RbohF, PR1* and *YLS9* (Figure 7a). To test whether WRKY42 can directly bind to the promoter regions of these target genes, we first performed an electrophoretic mobility shift assay (EMSA) using unlabeled probes as competitors and glutathione-*S*-transferase (GST) as the control protein. The results revealed that WRKY42 protein tagged with GST (GST-WRKY42) bound to probe 1 (P1) of the *SAG13*, *SAG24*, *SAG103*, *ICS1*, *PR1*, *RbohF* and *YLS9* promoters, and to P2 of the *PBS3* promoter, whereas GST alone could not bind to the promoters (Figure 7b–i). Competitive binding assays were also performed to confirm binding specificity by adding an excess of unlabeled probes, which competed with the labeled binding in all cases (Figure 7b–i). GST-WRKY42 did not bind to the other probes in the promoters of these eight genes, however (Figure S9). Moreover, to confirm binding, we further conducted a competitive assay using both unlabeled and mutant probes harboring mutations in the W-box of *ProICS1* and *ProRbohF* (Figure S10). The results showed that an excess of unlabeled native probes showed good competition, whereas mutant probes did not, which indicates that WRKY42 binds to the target genes through the W-box (Figure S10).

We next employed chromatin immunoprecipitation (ChIP) to further test the affinity of WRKY42 for its target gene promoters. For this assay, 2-week-old *WRKY42-HA* transgenic seedlings were used, and age-matched *wrky42-1* mutant seedlings were used as the control.

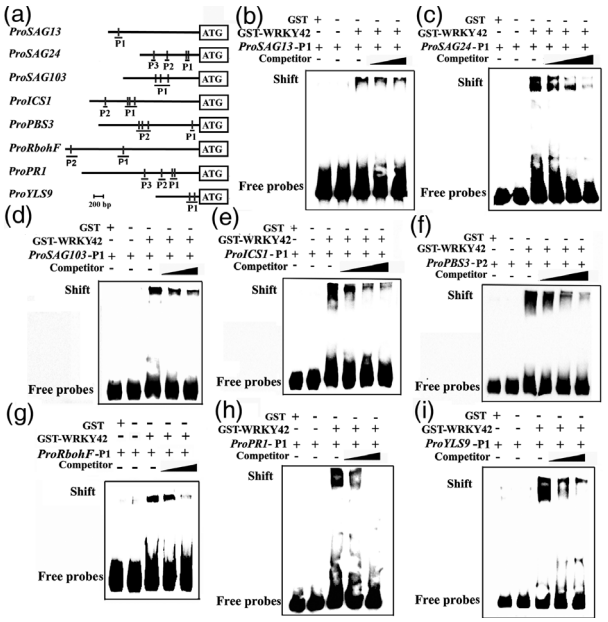

Figure 7. Electrophoretic mobility shift assays (EMSA) of WRKY42 binding to different regions of promoters of putative target genes.
(a) Schematic representation of *SAG13, SAG24, SAG103, ICS1, PBS3, RbohF, PR1* and *YLS9* promoter regions containing W-box *cis*-elements. Only canonical W-boxes (TTGACC/T, black vertical bars) are represented. The approximate positions of W-boxes relative to ATG start codon in respective promoters are indicated. The lines below W-boxes indicate the probes used in EMSA. (b–i) Competitive EMSA to detect the binding of WRKY42 to promoters of target genes. The DNA binding assays were performed using purified GST-WRKY42 protein and biotin-labelled fragments of the promoters containing the W-boxes, using GST protein as a negative control, and non-labeled fragments were used as competitors. The + and − symbols indicate the presence and absence of components. The bands at the upper and lower part of membranes indicate shift (protein-probe complex) and unbound free probes, respectively.

Immunoblotting and agarose gel electrophoresis assays indicated the utility of the anti-HA antibody and the good quality of sonicated chromatin DNA, respectively (Figure S11). Primers for each of the putative binding sites were designed to flank promoter regions that contained W-box elements and that had shown positive bindings in the EMSA assay (Figure 8a). The ChIP-qPCR results showed that WRKY42 significantly enriched the fragments containing F_1 of *ProSAG13* (Figure 8b), F_1 and F_3 of *ProSAG24* (Figure 8c), F_2 of *ProSAG103* (Figure 8d), F_1 and F_2 of *ProICS1* (Figure 8e), F_1–F_3 of *ProPBS3* (Figure 8f), F_1 and F_2 of *ProRbohF* (Figure 8g), F_1–F_3 of *ProPR1* (Figure 8h) and F_1 of *ProYSL9* (Figure 8i), whereas WRKY42 did not show any binding to the promoter of *ACTIN2* and the CF controls of different target genes (Figure 8b–i).Our results from both *in vitro* and *in vivo* assays therefore consistently indicated that WRKY42 directly binds to the promoters of *SAG13*, *SAG24*, *SAG103*, *ICS1*, *PBS3*, *PR1*, *RbohF* and *YLS9*.

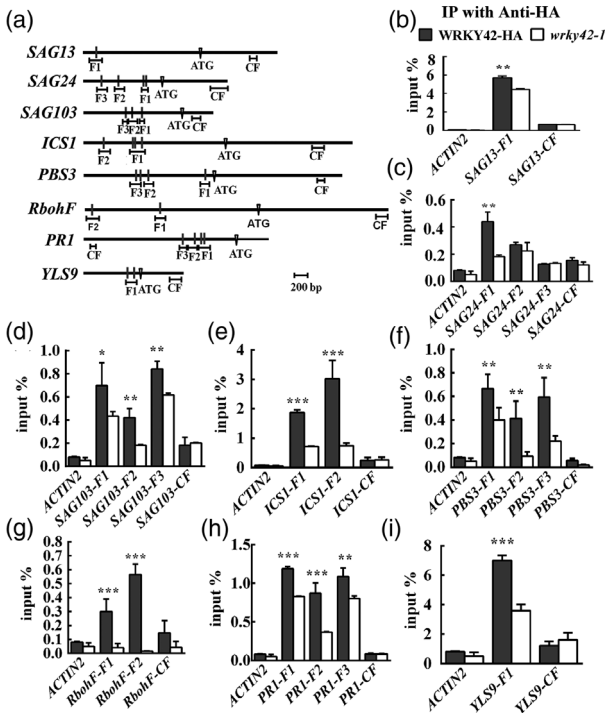

Figure 8. Chromatin immunoprecipitation (ChIP)-qPCR assay to examine the association between WRKY42 and its targets.
(a) Schematic diagrams of W-box elements in promoter regions of *SAG13, SAG24, SAG103, ICS1, PBS3, PR1* and *YLS9* genes with control primers in the coding regions or intergenic regions indicated by CF. Only perfect W-boxes (TTGACC/T, black vertical bars) are represented. ATG represents the translational start codon. The lines below W-boxes and CF indicate the sequences detected in ChIP-qPCR assay. (b–i) Association of WRKY42 with its targets by ChIP-qPCR assay. Chromatin prepared from 14-day-old *WRKY42-HA* plants using anti-HA antibody (IP) were detected with qPCR with chromatins prepared from *wrky42-1* as the control. Enrichment of specific fragments is expressed as percentage of input. *ACTIN2* promoter was also detected as a negative control. Data are means ± SE of four independent biological replicates. Statistical analysis was performed with Student's *t*-test (**P* < 0.05, ***P* < 0.01, ****P* < 0.001).

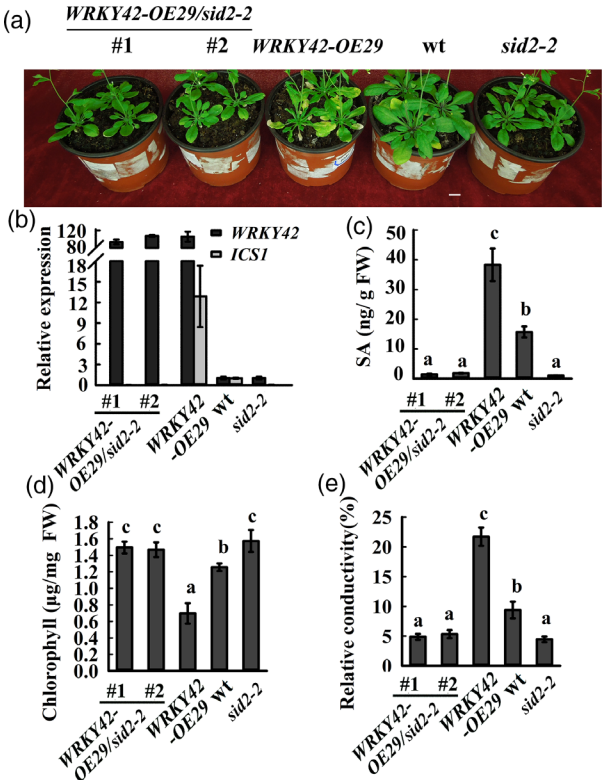

Figure 9. Mutation of *SID2* suppresses the early senescence phenotype of *WRKY42*-overexpressing plants.
(a) Leaf senescence phenotype of 35-day-old *WRKY42-OE29/sid2-2* #1, #2, *WRKY42-OE29,* wt and *sid2-2* plants. (b) qRT-PCR analysis of *WRKY42* and *ICS1/SID2* transcript levels in rosette leaves of plants shown in (a). Data are means ± SE of three independent biological replicates. Transcript levels of genes in wt were arbitrarily set to 1. (c–e) Measurements of free SA contents (c), chlorophyll contents (d) and relative conductivity (e) in the 5th-8th rosette leaves. Data are means ± SE of three to four independent biological replicates. Identical and different letters represent non-significant and significant differences ($P < 0.05$).

Mutation of *ICS1* suppresses the early leaf senescence phenotype of *WRKY42*-overexpressing plants

As our previous data indicate that WRKY42 induced leaf senescence through positively regulating ROS and SA synthesis, we determined to provide genetic evidence. Being a critical enzyme involved in SA synthesis (Wildermuth *et al.*, 2001), ICS1 (also called SID2) was chosen first. We generated *WRKY42-OE29/sid2-2* plants to investigate whether ICS1 was responsible for the increased SA level and accelerated leaf senescence evoked by the expression of *WRKY42*. We crossed the *WRKY42-OE29* transgenic line with a *sid2-2* mutant and obtained F_3 *WRKY42-OE29/sid2-2* plants. Again, seeds of different genotypes were harvested at the same time and under the same growth conditions before being used for phenotypic comparison. The expression of *WRKY42* and *ICS1* in the different genotypes was tested by qRT-PCR and the expected results were seen (Figure 9b). Under normal growth conditions, *WRKY42-OE29/sid2-2* plants showed an obvious delayed senescence phenotype compared with the *WRKY42-OE29* line (Figure 9a). Moreover, the mutation of *ICS1* also abolished the increased SA levels in the *WRKY42-OE29* background, and the free SA level in *WRKY42-OE29/sid2-2* plants was similar to that in the *sid2-2* mutant (Figure 9c). A higher chlorophyll content and lower relative conductivity further confirmed the delayed senescence phenotype in *WRKY42-OE29/sid2-2* plants (Figure 9d,e). Taken together, our results above suggest that the mutation of *ICS1* abolished the early senescence phenotype in *WRKY42-OE* lines by reducing the SA level and, hence, a positive regulatory module is proposed in which WRKY42-ICS1 modulates SA biosynthesis and thereby leaf senescence.

RbohF mutation suppresses the early senescence phenotype of *WRKY42*-overexpression plants

As *WRKY42* overexpression promotes H_2O_2 accumulation and also binds strongly to the W-box element in the promoter of *RbohF*, and activates its expression, we decided to explore the genetic relationship between RbohF and WRKY42. Loss-of-function mutants of *rbohf* had delayed senescence compared with the wt (Figure 10a). Plants with the combined *WRKY42-OE29/rbohf* genotype also had delayed senescence, compared with *WRKY42-OE29* (Figure 10a). Transcript abundance of *WRKY42* and *RbohF* was measured and was found to be consistent with the respective genotypes (Figure 10b). Furthermore, H_2O_2 concentration in *WRKY42-OE29/rbohf* plants was significantly lower than in *WRKY42-OE29* plants, and the H_2O_2 content in the *rbohf* mutant was significantly lower than that of the wt (Figure 10c). Finally, the higher chlorophyll content and lower relative conductivity in the *WRKY42-OE29/rbohf* plants further confirmed the delayed senescence phenotype (Figure 10d,e). These results suggest that mutation of *rbohf* suppressed the early senescence phenotype caused by *WRKY42* overexpression, by suppressing H_2O_2 accumulation. Hence, a WRKY42-RbohF pathway modulates ROS-dependent leaf senescence.

Higher levels of SA and H_2O_2 inhibit the expression of *WRKY42*

According to the above results, mutations of *ICS1* and *RbohF* suppress the early leaf senescence phenotype of *WRKY42*-overexpressing plants. It was interesting to find that the H_2O_2 content in *WRKY42*-OE/*sid2-2* plants was significantly decreased compared with the *WRKY42*-OE29 line (Figure S12a). Similarly, the SA content in *WRKY42*-OE29/*rbohf* plants was also significantly lower than that of *WRKY42*-OE29 plants (Figure S12b). These results suggest that SA and H_2O_2 levels are highly correlated, at least in *WKRY42*-overexpression plants.

Next, we further explored the influence of SA and H_2O_2 on the expression of *WRKY42* via qRT-PCR. The results showed that the expression of *WRKY42* was significantly reduced under 10 mM H_2O_2 and 500 μM SA treatments at 1, 3 and 12 h, whereas lower concentrations of H_2O_2 and SA had no such effect (Figure S13). Thus, *WRKY42* overexpression can accelerate SA and H_2O_2 accumulation through directly regulating the transcription of *ICS1* and *RbohF*; however, its own expression was suppressed by high levels of SA and H_2O_2, which forms a complex negative feedback network to fine-tune leaf senescence and growth in Arabidopsis.

DISCUSSION

Leaf senescence is the last stage of leaf development and is crucial for plant reproduction, fitness and adaptation to various environments (Schippers *et al.*, 2015). Dissecting the molecular mechanisms underlying leaf senescence may provide the theoretical basis for breeding more productive and environmentally adaptable varieties, as some functional stay-green mutants were found to have the potential to increase plant productivity (Thomas and Howarth, 2000; Yoo *et al.*, 2007; Hortensteiner, 2009). During the past decades, transcriptomic analyses have defined a large number of genes as *SAG*s, but only a small portion of them have been functionally characterized. In this study, we identified a novel positive regulator WRKY42 that functions in the onset of age-dependent leaf senescence.

Our study demonstrated that *WRKY42* exhibited high expression levels in senescent leaves compared with young leaves (Figure 1), implying that WRKY42 acts as a functional sen-TF. Overexpression of *WRKY42* dramatically accelerated leaf senescence at several developmental stages examined, whereas loss-of-function mutation of *WRKY42* delayed leaf senescence (Figures 2, 3, S2 and S3),

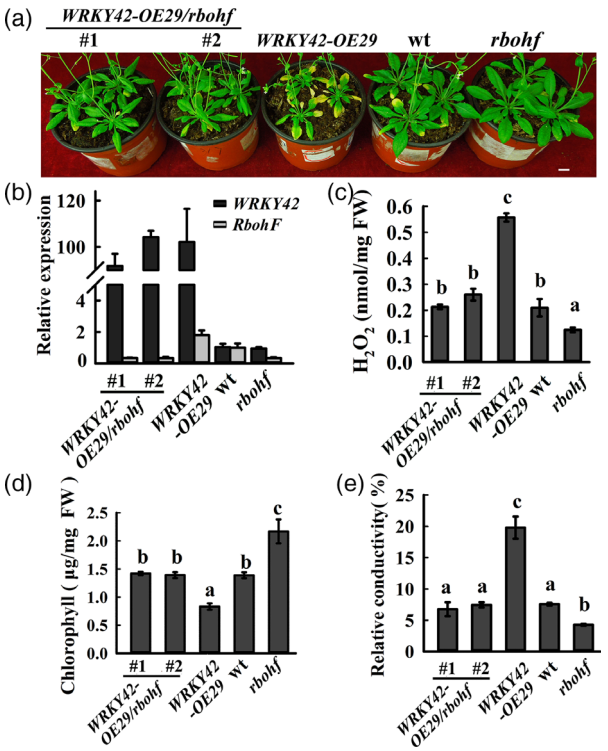

Figure 10. *RbohF* mutation suppresses the early senescence phenotype of *WRKY42*-overexpressing plants.
(a) Leaf senescence phenotype of 35-day-old *WRKY42-OE29/rbohf* #1, #2, *WRKY42-OE29,* wt and *rbohf* plants. (b) qRT-PCR analysis of *WRKY42* and *RbohF* transcript levels in rosette leaves of plants shown in (a). Data are means ± SE of four independent biological replicates. Transcript levels of genes in wt were arbitrarily set to 1. (c–e) Measurements of H_2O_2 contents (c), chlorophyll contents (d) and relative conductivity (e) in the 5th-8th rosette leaves. Data are means ± SE of three to four independent biological replicates. Identical and different letters represent non-significant and significant differences ($P < 0.05$).

further supporting its SAG function. Interestingly, altering the expression of *WRKY42* affected the progression of leaf senescence but had no influence on the seed mass per plant (Figure S4), demonstrating that overexpression of *WRKY42* can shorten the life cycle of transgenic Arabidopsis without affecting its yield at all. An RNA-seq profiling of differentially expressed genes between *WRKY42-OE29* and the wt (Col-0) uncovered an array of genes implicated in the synthesis and signaling of senescence-associated phytohormones and ROS, as well as many well-known SAGs and TF genes (Figure 4). Therefore, WRKY42 functions during leaf senescence by regulating the expression of many *SAG*s. Among the SAGs, *SAG13*, *SAG24* and *SAG103* showed opposite expression patterns in *wrky42* mutants and overexpression lines (Figure 5), and promoters of these were found to contain at least one canonical W-box element. Our EMSA and ChIP experiments demonstrated that WRKY42 bound directly to the *SAG13*, *SAG24* and *SAG103* promoters, indicating that these SAGs are direct targets of WRKY42. A more recent report also identifies *SAG12* and *SAG13* as a direct target of WRKY45 in age-triggered leaf senescence through a gibberellin-mediated signaling pathway (Chen *et al.*, 2017). *SAG12* was not found among the DEGs in our RNA-seq analysis, however.

WRKY6 is the first *WRKY* gene reported to regulate leaf senescence in Arabidopsis; however, the genetic evidence of the regulatory components, such as *SIRK*, is not clear (Robatzek and Somssich, 2001; Robatzek and Somssich, 2002). As the closest homolog of *WRKY6*, we provided experimental evidence to show the positive role played by WRKY42 here. Furthermore, *SIRK*, one target gene of WRKY6, was also indicated as a candidate target of WRKY42 (Figures 5 and 6). Previously, WRKY6 and WRKY42 were shown to play similar roles in response to low Pi stress by regulating *PHOSPHATE 1* (*PHO1*) expression (Chen *et al.*, 2009; Su *et al.*, 2015). These reports suggest that both WRKY6 and WRKY42 participate in the fine-tuning of signaling and regulatory network of leaf senescence and nutrient starvation responses.

A transcriptomic comparison between *WRKY42* overexpression and wild-type plants revealed the enrichment of SA, ROS, and abiotic and biotic stress-related biological processes, and a large portion of the genes involved in these processes are upregulated in *WRKY42*-overexpressing plants (Figure S5). In line with this finding, we found that free SA and H_2O_2 levels were dramatically increased in *WRKY42-OE* lines but decreased in the *wrky42* mutant plants (Figures 2, 3 and S7). As SA and H_2O_2 are two well-defined inducers of leaf senescence and longevity (Khanna-Chopra, 2012; Zhang *et al.*, 2013), we focused on dissecting the molecular mechanisms mediated by WRKY42. Three putative target genes involved in SA biosynthesis and H_2O_2 production were identified within the RNA-seq results: *ICS1*, *PBS3* and *RbohF*. *ICS1* is a key gene responsible for SA biosynthesis (Dempsey *et al.*, 2011), but its role in natural senescence is not well established. Our study indicates that *ICS1* is a direct target of WRKY42 (Figures 7 and 8), and genetic evidence further demonstrates that the mutation of *ICS1* repressed the SA accumulation and early senescence phenotype of *WRKY42*-overexpressing plants (Figure 9). From these results, we concluded that WRKY42 promotes SA production and leaf senescence partially by inducing *ICS1* expression.

Previous studies have revealed H_2O_2 as an important signaling molecule that plays an essential role in many different process, including plant senescence (Lee *et al.*, 2012; Guo *et al.*, 2017; Waszczak *et al.*, 2018). In Arabidopsis, there are 10 *Rboh* genes that may play a role in a tissue or organ-specific manner (Torres and Dangl, 2005; Suzuki *et al.*, 2011; Daniel *et al.*, 2012). Although some of them may function redundantly, their tissue-specific expression also suggests their functional specialization (Steinhorst and Kudla, 2013; Morales *et al.*, 2016). In this study, we found that one of the *Rboh*s, *RbohF*, was directly upregulated by WRKY42. RbohF is a multifunctional NADPH oxidase that participates in diverse physiological processes (Chaouch *et al.*, 2012; Yuree *et al.*, 2013; Morales *et al.*, 2016); however, the TFs that regulate the expression of *RbohF* expression have not been reported. Our study reveals that WRKY42 acts as an upstream factor of *RbohF* expression to determine leaf senescence progression (Figure 10). Previous studies have shown that AtRbohF may function redundantly with RbohD in defense against pathogens, cell-death control and ABA-induced stomatal closure, as the double mutant *rbohd rbohf* demonstrates a stronger phenotype (Kwak *et al.*, 2003; Torres *et al.*, 2005). *RbohD* was not identified to be differentially expressed in our RNA-seq data, however. Later, it was found that RbohF also has a specific role in protecting shoot cells from excessive Na^+ (Jiang *et al.*, 2012).

In summary, our study has identified WRKY42 as a novel transcription factor in the senescence regulatory network, through directly regulating the transcription of *ICS1* and *RbohF* to promote SA and H_2O_2 accumulation, as well as several well-known *SAG*s and *YLS9*. We therefore propose a working model for the function of WRKY42 in integrating ROS and SA signaling to control the onset and progression of leaf senescence (Figure S14). In the future, it will be interesting to determine whether this mechanism is applicable to other WRKY TFs and how WRKY42 regulates the expression of other putative target genes uncovered from the RNA-seq analysis.

EXPERIMENTAL PROCEDURES

Plant materials and growth conditions

The *Arabidopsis thaliana* ecotype Columbia (Col-0) was used as the wt for this study. T-DNA insertion mutants of *wrky42-1*

(Salk_121674), *wrky42-2* (Salk_203446), *rbohf* (Salk_034674), *pbs3* (Salk_018225) and *sid2-2* (Dewdney *et al.*, 2000) were ordered from the Arabidopsis Biological Resource Center (ABRC, https://abrc.osu.edu) and Nottingham Arabidopsis Stock Center (NASC, http://arabidopsis.info).

Seeds were surface-sterilized and plated on half-strength Murashige and Skoog (MS) medium with 1% sucrose and 0.8% Phytoblend (Caissonlabs, https://www.caissonlabs.com), stratified at 4°C for 2 days, and then transferred to a growth chamber with 14-h light/10-h dark cycle at 22°C, and a light intensity of approximately 120 μmol m^{-2} sec^{-1}, with a relative humidity of 60–70%. Homozygous mutants were screened by PCR and expression levels were determined by RT-PCR.

Construction of transgenic overexpression lines

To generate *Pro35S:WRKY42-HA*-overexpression lines, the coding region of *WRKY42* was amplified using high-fidelity PrimeSTAR HS DNA polymerase (TaKaRa, https://www.takarabio.com) with the primers listed in Table S1 before being cloned into the previously described binary vector pYJHA (Niu *et al.*, 2016) to obtain the pYJHA-*WRKY42* with a 2 × HA tag at the 3′ end. For generating the *Pro35S:GFP-HA* control lines, *GFP* was constructed into pYJHA separately. After confirmation, both constructs were individually transformed into the wt (Col-0) through *Agrobacterium*-mediated floral dip (Clough and Bent, 1998). The transformants were selected on half-strength MS medium supplemented with 1% sucrose and 25 μg ml^{-1} hygromycin B. High expression lines were identified through qRT-PCR and confirmed by Western blot. Homozygous T_3 lines were used for phenotypic and qRT-PCR assays.

Quantitative RT-PCR (qRT-PCR) assay

Total RNA was extracted from leaves of different ages or age-matched rosette leaves of triplicates using the Plant RNA kit and treated with RNase-free DNase (Omega Bio-tek, https://www.omegabiotek.com) according to the manufacturer's instructions. Reverse transcription was performed with 2.5 μg of total RNA in a 20-μl reaction mixture using H^-MMLV reverse transcriptase and oligo $(dT)_{18}$ (TaKaRa). Ten-fold diluted cDNA samples were then used as templates for qRT-PCR, using SYBR Premix Ex Taq (TaKaRa) on the CFX96 real-time thermocycler (Bio-Rad, https://www.bio-rad.com). *UBQ10* and *UBC21* were used as internal controls to normalize expression levels of target genes (Jiang and Deyholos, 2009). The primers used are listed in Table S1.

For H_2O_2 and SA treatments, 10-day-old wt (Col-0) seedlings grown on half-strength MS medium were transferred to half-strength MS medium containing 1 or 10 mM H_2O_2 (Alfa Aesar, http://www.alfa.com), 50 or 500 μM SA (Sigma-Aldrich, https://www.sigmaaldrich.com), respectively. Seedlings transferred to normal half-strength MS medium were used as the control. Seedlings were harvested at 1, 3 and 12 h after treatments, flash-frozen in liquid nitrogen and stored at −80°C. The planting, treatments and harvesting were repeated three times independently. Then RNA extraction and qRT-PCR were performed with the primers listed in Table S1.

Protein extraction and Western blot assay

To analyze the expression levels of HA-tagged WRKY42 and GFP proteins in transgenic lines, total proteins from rosette leaves were extracted in a lysis buffer (0.7 M sucrose, 500 mM Tris-HCl, pH 7.5, 50 mM EDTA-Na, pH 8.0, 0.1 M KCl, 1.0% Triton X-100, full-strength protease inhibitor cocktail; Pierce, now ThermoFisher Scientific, https://www.thermofisher.com). For immunoblot analysis, equal quantities of proteins were separated on a 10% SDS-PAGE gel, followed by target protein detection with anti-HA (1:2000) antibody (Sigma-Aldrich) and horseradish peroxide (HRP)-conjugated secondary antibody (Pierce, https://www.thermofisher.com/). The chemiluminescence signals were visualized using a SuperSignal West Pico PLUS Chemiluminescent substrate (Pierce, now ThermoFisher Scientific) on a ChemDoc system (Bio-Rad), according to the manufacturer's instructions.

Promoter-β-glucuronidase (GUS) fusion and histochemical staining

To construct *ProWRKY42:GUS*, a 2-kb genomic sequence upstream of the *WRKY42* start codon was amplified from genomic DNA and inserted into a modified linearized pRD420 vector (Datla *et al.*, 1992), in which the original GUS gene was replaced with intron-containing GUS from pCAMBIA1391Z. The construct was confirmed by DNA sequencing and then transformed into Arabidopsis Col-0, as described above. Seeds were selected on half-strength MS medium containing 25 μg ml^{-1} kanamycin. Homozygous T_2 lines were used for GUS staining, as described previously (Jiang and Deyholos, 2009). Over 10 independent seedlings grown in half-strength MS medium or soil were subjected to staining and displayed similar staining patterns. Representative data are shown.

Leaf senescence assays

Seeds of different genotypes were harvested from plants grown at the same time and under the same growth conditions. For phenotypic assay, seeds were germinated on half-strength MS medium supplemented with 1% sucrose for 7 days and then seedlings were transferred into soil and continued to grow under the same conditions. Age-matched rosette leaves among different genotypes were used for the leaf senescence assay. Leaves 5–8 from 35-day-old plants were used for measurements of chlorophyll content, relative conductivity and H_2O_2 content, as described previously (Chen *et al.*, 2016). In addition, the rosette leaves 5–9 were subjected to DAB staining (Sun *et al.*, 2014).

Hormone measurements

The rosette leaves of various genotypes from soil-grown plants were used and four biological replicates were prepared for each genotype. Approximately 200 mg of fresh leaf sample for each genotype was collected and flash-frozen in liquid nitrogen, with hormone concentrations detected using a previously described protocol (Wu *et al.*, 2007; Yang *et al.*, 2012). In brief, 1 ml ethyl acetate containing 200 ng of $^2H_4$-SA, ^{6}H-ABA and D_6-JA used as internal standards for SA, ABA and JA respectively, were added to each sample. Samples were then homogenized using a FastPrep homogenizer (ThermoFisher Scietific). Next, the homogenized samples were centrifuged at 16 100 ***g*** for 10 min at 4°C and the supernatants were transferred to 2-ml tubes. The precipitate was extracted with 0.5 ml of ethyl acetate again, and the supernatants were combined and evaporated to dryness using a vacuum concentrator (Eppendorf, https://www.eppendorf.com). The residue of each sample was resuspended in 0.5 ml of 70% methanol (v/v), centrifuged at 16 100 ***g*** for 15 min and the supernatants were transferred into glass vials and used for hormone detection. The analyses of SA, ABA and JA were performed on an ultra-performance liquid chromatography (UPLC) system with a Shim-pack XR-ODS (2.0 mm I.D. × 75 mm L.,1.6 μm) column coupled to a triple quadrupole mass spectrometer (LC-MS8040; Shimazu, https://www.shimadzu.com) with an electrospray source (ESI).

RNA-seq assay

Rosette leaves 7 and 8 of 30-day-old wt (Col-0) and *WRKY42-OE29* plants were individually collected from plants of three biological replicates, frozen in liquid nitrogen and stored at −80°C. The RNA-seq analysis was performed by CapitalBio Technology Inc. (http://www.capitalbiotech.com), with three biological replicates. Briefly, RNA quality was evaluated on an Agilent 2100 BioAnalyzer (Agilent, https://explore.agilent.com). Sequencing libraries were generated following the manufacturer's protocol of NEBNext Ultra RNA Library Prep Kit for Illumina (#E7530S; New England Biolabs, https://international.neb.com). After quality control and cluster generation, the sequencing was performed on an Illumina HiSeq 2000 platform. The FastQC (Wingett and Andrews, 2018) and NGSQC (Patel and Jain, 2012) were used to evaluate and filter the raw data. The high-quality filtered reads were then mapped to Arabidopsis reference genome (TAIR10) with TOPHAT. DEG analysis was performed using CUFFDIFF. Genes with $|\log_2 FC| \geq 1$ and $P < 0.05$ were identified as DEGs. GO enrichment analysis was conducted by using BINGO (https://www.psb.ugent.be/cbd/papers).

Dual luciferase reporter assay

Promoters of individual target genes were amplified from Arabidopsis genomic DNA and cloned into the transient expression vector pGreenII0800-LUC to serve as the reporter plasmids. The individual promoters were inserted into upstream of firefly luciferase (LUC) gene and the *Renilla* luciferase (REN) gene under the control of the CaMV 35S promoter was used as the endogenous control (Hellens *et al.*, 2005). The pYJHA-*WRKY42* was used as an effector plasmid, with pYJHA-*GFP* used as a negative control plasmid. The effector plasmids and reporter plasmids were transformed into *Agrobacterium tumefaciens* GV3101 (pSoup) individually. The effector and the reporter plasmids were then mixed at a ratio of 9:1(v/v), and then infiltrated into the 28 days old *N.benthamiana* leaves. At 2 and 3 dpi (day post-infiltration), three leaf discs of 1 cm in diameter were harvested and the dual luciferase reporter assay was performed using the Dual-Luciferase Reporter Assay System kit (Promega, USA, https://www.promega.com/) according to manufacturer's instructions. Primers used are listed in Table S1.

Electrophoretic mobility shift assay (EMSA)

The coding region of *WRKY42* was amplified and cloned into pGEX4T-1 vector. The GST-WRKY42 fusion protein and GST (as the control) were expressed in *E. coli* strain Rosetta (DE3) (Novagen, Germany, http://www.merckmillipore.com). The recombinant proteins were induced with 0.2 mM isopropyl-β-D-1-thiogalactopyranoside (IPTG) at 25°C for 4 h and purified with GST-bind resin (Novagen) following the manufacturer's instructions. EMSA was performed using the Light Shift Chemiluminescent EMSA Kit (Pierce, USA, https://www.thermofisher.com/) according to the manufacturer's instructions. The oligonucleotide sequences and primers of biotin-labeled probes, unlabeled probes and mutant probes are listed in Table S1.

ChIP-qPCR assay

Two-week-old *WRKY42-HA* transgenic seedlings and *wrky42-1* mutant seedlings were used as materials according to (Saleh *et al.*, 2008). In brief, about 3 g seedlings were collected and cross-linked with 1% formaldehyde (Sigma-Aldrich) under a vacuum for 10 min. The reaction was stopped by adding glycine at a final concentration of 100 mM for another 5 min. Then the samples were washed twice with distilled water and frozen in liquid nitrogen. Next, the chromatin DNA was isolated, sonicated and then precleared with salmon sperm DNA/protein A agarose beads (Upstate, USA, http://www.merckmillipore.com) for 1 h. Afterwards immunoprecipitation was performed with HA antibody (#H6908, Sigma-Aldrich) at 4°C overnight with gentle rotation. The immunoprecipitated complexes were then precipitated with salmon sperm DNA/protein A agarose beads at 4°C with gentle rotation for 4 h. Finally, the precipitated DNA was recovered after reverse cross-linking and protein digestion, and then analyzed by quantitative PCR (qPCR). The precipitated chromatin DNA of *wrky42-1* mutant was used as the negative control, while sonicated chromatin DNA without precipitation served as an input control. For data analysis, ChIP results are presented as a percentage of input DNA. *ACTIN2* and gene-specific primers annealing to regions located at least 1 kb downstream of the translational start site were used as controls. Primers used are listed in Table S1.

Statistical analysis

All experiments were repeated with at least three biological replicates. All presented data were statistically analyzed by using SPSS 16.0 software.

ACCESSION NUMBERS

RNA-seq raw data are available at the Sequence Read Archive (SRA) database (https://dataview.ncbi.nlm.nih.gov/) under the accession number SUB5690510. Sequence data from this article can be found in the TAIR website (https://www.arabidopsis.org) under the following AGI codes: *WRKY42* (AT4G04450), *ICS1* (AT1G74710), *RbohF* (AT1G64060), *SAG13* (AT2G29350), *SAG21* (AT4G02380), *SAG24* (AT1G66580), *SAG101* (AT5G14930), *SAG103* (AT1G10140), *YLS9* (AT2G35980), *ZAT12* (AT5G59820), *ACS2* (AT1G01480), *ACS6* (AT4G11280), *NCED4* (AT4G19170), *NCED5* (AT1G30100), *LOX1* (AT1G55020), *LOX5* (AT3G22400), *PBS3* (AT5G13320), *SIRK* (AT2G19190), *PR1* (AT2G14610), *PR5* (AT1G75040), *PDF1.4* (AT1G19610), *PDF2.1* (AT2G02120), *ATG8E* (AT2G45170), *MC2* (AT4G25110), *MC6* (AT4G25111), *MC8* (AT1G16420), *IAA1* (AT4G14560), *PIN1* (AT1G73590), *ELIP1* (AT3G22840), *LDOX* (AT4G22880), *UBQ10* (AT4G05320), *UBC21* (AT5G25760) and *ACTIN2* (AT3G18780).

ACKNOWLEDGEMENTS

This research was supported by the National Natural Science Foundation of China (31270293, 31771699 to YQJ, 31301648 to BY) and the Fundamental Research Funds for the Central Universities (2452017025 to YQJ, 2452019067 to BY), and Open Project of State Key Laboratory of Plant Physiology and Biochemistry (SKLPPBKF2001 to YQJ), and the Natural Sciences and Engineering Research Council Discovery grant of Canada (to MKD). We thank ABRC and NASC for providing the mutant seeds, Drs Jian-Qiang Wu and Jinfeng Qi (Kunming Institute of Botany, CAS) for technical help.

AUTHOR CONTRIBUTIONS

YQJ and BY conceived, designed and supervised the research; FN, BY and YQJ performed most of the experiments; XC, PZ, MS, YL and XZ helped the material preparation and experiments; FN, BY, YQJ and MKD analyzed the

data; YQJ, BY and FN wrote the article with inputs from MKD. All authors reviewed and approved the manuscript.

CONFLICT OF INTEREST

The authors declare that they have no conflicts of interest with the contents of this article.

SUPPORTING INFORMATION

Additional Supporting Information may be found in the online version of this article.

Figure S1. Domain organization, subcellular localization and protein-protein interaction of WRKY42.

Figure S2. *WRKY42* overexpression lines show accelerated leaf senescence phenotype at 30 days old.

Figure S3. Age-dependent leaf senescence phenotype of *WRKY42* overexpression and mutant plants.

Figure S4. qRT-PCR analysis of the transcript level of senescence marker gene *SAG12* in different genotypes.

Figure S5. Comparison of seed mass of *WRKY42*-related genotypes.

Figure S6. Functional categorization of the DEGs (differentially expressed genes) by gene ontology (GO) analysis from transcriptome sequencing.

Figure S7. Dual luciferase (LUC) reporter analysis of senescence-related genes identified through RNA-seq.

Figure S8. WRKY42 positively regulates the accumulation of phytohormones.

Figure S9. Electrophoretic mobility shift assays (EMSA) of the binding of WRKY42 to the promoter fragments of putative target genes.

Figure S10. Competitive electrophoretic mobility shift assays (EMSA) of the binding of WRKY42 to the promoter fragments of *ICS1* and *RbohF*.

Figure S11. Western blot analysis of WRKY42 protein and agarose gel electrophoresis analysis of fragmented chromatin of *WRKY42-OE29* plants for ChIP assay.

Figure S12. Quantitative analysis of H_2O_2 and SA contents in *WRKY42*-OE/*sid2-2* and *WRKY42*-OE/*rbobf* lines.

Figure S13. qRT-PCR analysis of *WRKY42* expression in response to H_2O_2 and SA treatments.

Figure S14. A working model illustrating AtWRKY42 functions in age-induced leaf senescence.

Table S1. Primers used in this study.

REFERENCES

Apel, K. and Hirt, H. (2004) Reactive oxygen species: metabolism, oxidative stress, and signal transduction. *Annu Rev. Plant Biol.* **55**, 373–399.

Balazadeh, S., Riano-Pachon, D.M. and Mueller-Roeber, B. (2008) Transcription factors regulating leaf senescence in Arabidopsis thaliana. *Plant Biol. (Stuttg)*, **10**(Suppl 1), 63–75.

Besseau, S., Li, J. and Palva, E.T. (2012) WRKY54 and WRKY70 co-operate as negative regulators of leaf senescence in Arabidopsis thaliana. *J. Exp. Bot.* **63**, 2667–2679.

Breeze, E., Harrison, E., McHattie, S. *et al.* (2011) High-resolution temporal profiling of transcripts during Arabidopsis leaf senescence reveals a distinct chronology of processes and regulation. *Plant Cell*, **23**, 873–894.

Chaouch, S., Queval, G. and Noctor, G. (2012) AtRbohF is a crucial modulator of defence-associated metabolism and a key actor in the interplay between intracellular oxidative stress and pathogenesis responses in Arabidopsis. *Plant J.* **69**, 613–627.

Chen, B., Niu, F., Liu, W.Z., Yang, B., Zhang, J., Ma, J., Cheng, H., Han, F. and Jiang, Y.Q. (2016) Identification, cloning and characterization of R2R3-MYB gene family in canola (*Brassica napus* L.) identify a novel member modulating ROS accumulation and hypersensitive-like cell death. *DNA Res.* **23**, 101–114.

Chen, L., Xiang, S., Chen, Y., Li, D. and Yu, D. (2017) Arabidopsis WRKY45 interacts with the DELLA protein RGL1 to positively regulate age-triggered leaf senescence. *Mol. Plant*, **10**, 1174–1189.

Chen, Y.F., Li, L.Q., Xu, Q., Kong, Y.H., Wang, H. and Wu, W.H. (2009) The WRKY6 transcription factor modulates PHOSPHATE1 expression in response to low Pi stress in Arabidopsis. *Plant Cell*, **21**, 3554–3566.

Clough, S.J. and Bent, A.F. (1998) Floral dip: a simplified method for Agrobacterium-mediated transformation of Arabidopsis thaliana. *Plant J.* **16**, 735–743.

Daniel, M., Christophe, D., Alain, P. and Nicolas, P. (2012) A burst of plant NADPH oxidases. *Trends Plant Sci.* **17**, 9–15.

Datla, R.S., Hammerlindl, J.K., Panchuk, B., Pelcher, L.E. and Keller, W. (1992) Modified binary plant transformation vectors with the wild-type gene encoding NPTII. *Gene*, **122**, 383–384.

Dempsey, D., Vlotb, A., Wildermuthc, M.C. and Klessiga, D. (2011) Salicylic acid biosynthesis and metabolism. *Arabidopsis Book*, **9**, e0156. 0110. 1199/tab.0156

Dewdney, J., Reuber, T.L., Wildermuth, M.C., Devoto, A., Cui, J., Stutius, L.M., Drummond, E.P. and Ausubel, F.M. (2000) Three unique mutants of Arabidopsis identify eds loci required for limiting growth of a biotrophic fungal pathogen. *Plant J.* **24**(2), 205–218.

Dong, J., Chen, C. and Chen, Z. (2003) Expression profiles of the Arabidopsis WRKY gene superfamily during plant defense response. *Plant Mol. Biol.* **51**, 21–37.

Eulgem, T., Rushton, P.J., Robatzek, S. and Somssich, I.E. (2000) The WRKY superfamily of plant transcription factors. *Trends Plant Sci.* **5**, 199–206.

Gan, S. and Amasino, R.M. (1997) Making sense of senescence (Molecular genetic regulation and manipulation of leaf senescence). *Plant Physiol.* **113**, 313–319.

Garcion, C., Lohmann, A., Lamodiere, E., Catinot, J., Buchala, A., Doermann, P. and Metraux, J.P. (2008) Characterization and biological function of the ISOCHORISMATE SYNTHASE2 gene of Arabidopsis. *Plant Physiol.* **147**, 1279–1287.

Gepstein, S., Sabehi, G., Carp, M.J., Hajouj, T., Nesher, M.F., Yariv, I., Dor, C. and Bassani, M. (2003) Large-scale identification of leaf senescence-associated genes. *Plant J.* **36**, 629–642.

Grbić, V. and Bleecker, A.B. (1995) Ethylene regulates the timing of leaf senescence in Arabidopsis. *Plant J.* **8**, 595–602.

Guo, P., Li, Z., Huang, P., Li, B., Fang, S., Chu, J. and Guo, H. (2017) A tripartite amplification loopinvolving the yranscription factor WRKY75, salicylic acid, and reactive oxygen species accelerates leaf senescence. *Plant Cell*, **29**, 2854–2870.

Guo, Y., Cai, Z. and Gan, S. (2004) Transcriptom of Arabidopsis leaf senescence. *Plant Cell Environ.* **27**, 521–549.

Guo, Y. and Gan, S. (2005) Leaf senescence: signals, execution, and regulation. *Curr. Top. Dev. Biol.* **71**, 83–112.

He, Y., Fukushige, H., Hildebrand, D.F. and Gan, S. (2002) Evidence supporting a role of jasmonic acid in Arabidopsis leaf senescence. *Plant Physiol.* **128**, 876–884.

Hellens, R.P., Allan, A.C., Friel, E.N., Bolitho, K., Grafton, K., Templeton, M.D., Karunairetnam, S., Gleave, A.P. and Laing, W.A. (2005) Transient expression vectors for functional genomics, quantification of promoter activity and RNA silencing in plants. *Plant Methods*, **1**, 13.

Hieno, A., Naznin, H.A., Inaba-Hasegawa, K. *et al.* (2019) Transcriptome analysis and identification of a transcriptional regulatory network in the response to H_2O_2. *Plant Physiol.* **180**, 1629–1646.

Hortensteiner, S. (2009) Stay-green regulates chlorophyll and chlorophyll-binding protein degradation during senescence. *Trends Plant Sci.* **14**, 155–162.

Jiang, C., Belfield, E.J., Mithani, A., Visscher, A., Ragoussis, J., Mott, R., Smith, J.A. and Harberd, N.P. (2012) ROS-mediated vascular homeostatic control of root-to-shoot soil Na delivery in Arabidopsis. *EMBO J.* **31**, 4359–4370.

Jiang, Y. and Deyholos, M.K. (2009) Functional characterization of Arabidopsis NaCl-inducible WRKY25 and WRKY33 transcription factors in abiotic stresses. *Plant Mol. Biol.* **69**, 91–105.

Jiang, Y., Liang, G., Yang, S. and Yu, D. (2014) Arabidopsis WRKY57 functions as a node of convergence for jasmonic acid- and auxin-mediated signaling in jasmonic acid-induced leaf senescence. *Plant Cell*, **26**, 230–245.

Khanna-Chopra, R. (2012) Leaf senescence and abiotic stresses share reactive oxygen species-mediated chloroplast degradation. *Protoplasma*, **249**, 469–481.

Kwak, J.M., Mori, I.C., Pei, Z.M., Leonhardt, N., Torres, M.A., Dangl, J.L., Bloom, R.E., Bodde, S., Jones, J.D. and Schroeder, J.I. (2003) NADPH oxidase AtrbohD and AtrbohF genes function in ROS-dependent ABA signaling in Arabidopsis. *EMBO J.* **22**, 2623–2633.

Lee, S., Seo, P.J., Lee, H.J. and Park, C.M. (2012) A NAC transcription factor NTL4 promotes reactive oxygen species production during drought-induced leaf senescence in Arabidopsis. *Plant J.* **70**, 831–844.

Leon, J., Lawton, M.A. and Raskin, I. (1995) Hydrogen peroxide stimulates salicylic acid biosynthesis in tobacco. *Plant Physiol.* **108**, 1673–1678.

Leshem, Y.Y. (1988) Plant senescence processes and free radicals. *Free Radic. Biol. Med.* **5**, 39–49.

Li, Z., Peng, J., Wen, X. and Guo, H. (2012) Gene network analysis and functional studies of senescence-associated genes reveal novel regulators of Arabidopsis leaf senescence. *J Integr. Plant Biol.* **54**, 526–539.

Lim, P.O., Kim, H.J. and Nam, H.G. (2007) Leaf senescence. *Annu. Rev. Plant Biol.* **58**, 115–136.

Mhamdi, A. and Van Breusegem, F. (2018) Reactive oxygen species in plant development. *Development*, **145**, 1–12.

Miao, Y., Laun, T., Zimmermann, P. and Zentgraf, U. (2004) Targets of the WRKY53 transcription factor and its role during leaf senescence in Arabidopsis. *Plant Mol. Biol.* **55**, 853–867.

Miller, G., Schlauch, K., Tam, R., Cortes, D., Torres, M.A., Shulaev, V., Dangl, J.L. and Mittler, R. (2009) The plant NADPH oxidase RBOHD mediates rapid systemic signaling in response to diverse stimuli. *Sci. Signal.* **2**, ra45.

Mittler, R. (2017) ROS are good. *Trends Plant Sci.* **22**, 11–19.

Morales, J., Kadota, Y., Zipfel, C., Molina, A. and Torres, M.A. (2016) The Arabidopsis NADPH oxidases RbohD and RbohF display differential expression patterns and contributions during plant immunity. *J. Exp. Bot.* **67**, 1663–1676.

Morris, K., MacKerness, S.A., Page, T., John, C.F., Murphy, A.M., Carr, J.P. and Buchanan-Wollaston, V. (2000) Salicylic acid has a role in regulating gene expression during leaf senescence. *Plant J.* **23**, 677–685.

Niu, F., Wang, C., Yan, J., Guo, X., Wu, F., Yang, B., Deyholos, M.K. and Jiang, Y.Q. (2016) Functional characterization of NAC55 transcription factor from oilseed rape (*Brassica napus* L.) as a novel transcriptional activator modulating reactive oxygen species accumulation and cell death. *Plant Mol. Biol.* **92**, 89–104.

Noh, Y.S. and Amasino, R.M. (1999) Identification of a promoter region responsible for the senescence-specific expression of SAG12. *Plant Mol. Biol.* **41**, 181–194.

Patel, R.K. and Jain, M. (2012) NGS QC Toolkit: a toolkit for quality control of next generation sequencing data. *PLoS One*, **7**, e30619.

Rao, M.V., Paliyath, G., Ormrod, D.P., Murr, D.P. and Watkins, C.B. (1997) Influence of salicylic acid on H_2O_2 production, oxidative stress, and H_2O_2-metabolizing enzymes. Salicylic acid-mediated oxidative damage requires H_2O_2. *Plant Physiol.* **115**, 137–149.

Rekhter, D., Lüdke, D., Ding, Y., Feussner, K., Zienkiewicz, K., Lipka, V., Wiermer, M., Zhang, Y. and Feussner, I. (2019) Isochorismate-derived biosynthesis of the plant stress hormone salicylic acid. *Science*, **365**, 498–502.

Robatzek, S. and Somssich, I.E. (2001) A new member of the Arabidopsis WRKY transcription factor family, AtWRKY6, is associated with both senescence- and defence-related processes. *Plant J.* **28**, 123–133.

Robatzek, S. and Somssich, I.E. (2002) Targets of AtWRKY6 regulation during plant senescence and pathogen defense. *Genes Dev.* **16**, 1139–1149.

Saleh, A., Alvarez-Venegas, R. and Avramova, Z. (2008) An efficient chromatin immunoprecipitation (ChIP) protocol for studying histone modifications in Arabidopsis plants. *Nat. Protoc.* **3**, 1018–1025.

Schippers, J.H., Schmidt, R., Wagstaff, C. and Jing, H.C. (2015) Living to die and dying to live: the survival strategy behind leaf senescence. *Plant Physiol.* **169**, 914–930.

Steinhorst, L. and Kudla, J. (2013) Calcium and reactive oxygen species rule the waves of signaling. *Plant Physiol.* **163**, 471–485.

Su, T., Xu, Q., Zhang, F.C., Chen, Y., Li, L.Q., Wu, W.H. and Chen, Y.F. (2015) WRKY42 modulates phosphate homeostasis through regulating phosphate translocation and acquisition in Arabidopsis. *Plant Physiol.* **167**, 1579–1591.

Sun, Y., Wang, C., Yang, B. *et al.* (2014) Identification and functional analysis of mitogen-activated protein kinase kinase kinase (MAPKKK) genes in canola (*Brassica napus* L.). *J. Exp. Bot.* **65**, 2171–2188.

Suzuki, N., Miller, G., Morales, J., Shulaev, V., Torres, M.A. and Mittler, R. (2011) Respiratory burst oxidases: the engines of ROS signaling. *Curr. Opin. Plant Biol.* **14**, 691–699.

Thomas, H. and Howarth, C.J. (2000) Five ways to stay green. *J. Exp. Bot.* **51**, 329–337.

Torrens-Spence, M.P., Bobokalonova, A., Carballo, V., Glinkerman, C.M., Pluskal, T., Shen, A., and Weng, J.-K. (2019) PBS3 and EPS1 Complete Salicylic Acid Biosynthesis from Isochorismate in Arabidopsis. *Molecular Plant*, **12**, 1577–1586.

Torres, M.A. and Dangl, J.L. (2005) Functions of the respiratory burst oxidase in biotic interactions, abiotic stress and development. *Curr. Opin. Plant Biol.* **8**, 397–403.

Torres, M.A., Dangl, J.L. and Jones, J.D. (2002) Arabidopsis gp91phox homologues AtrbohD and AtrbohF are required for accumulation of reactive oxygen intermediates in the plant defense response. *Proc. Natl. Acad. Sci. USA*, **99**, 517–522.

Torres, M.A., Jones, J.D. and Dangl, J.L. (2005) Pathogen-induced, NADPH oxidase-derived reactive oxygen intermediates suppress spread of cell death in Arabidopsis thaliana. *Nat. Genet.* **37**, 1130–1134.

Van Breusegem, F. and Dat, J.F. (2006) Reactive oxygen species in plant cell death. *Plant Physiol.* **141**, 384–390.

Waszczak, C., Carmody, M. and Kangasjarvi, J. (2018) Reactive oxygen species in plant signaling. *Annu. Rev. Plant Biol.* **69**, 209–236.

Wildermuth, M.C., Dewdney, J., Wu, G. and Ausubel, F.M. (2001) Isochorismate synthase is required to synthesize salicylic acid for plant defence. *Nature*, **414**, 562–565.

Wingett, S.W., and Andrews, S. (2018) FastQ Screen: A tool for multi-genome mapping and quality control. *F1000Research*, **7**, 1338.

Woo, H.R., Kim, H.J., Nam, H.G. and Lim, P.O. (2013) Plant leaf senescence and death - regulation by multiple layers of control and implications for aging in general. *J. Cell Sci.* **126**, 4823–4833.

Woo, H.R., Koo, H.J., Kim, J. *et al.* (2016) Programming of plant leaf senescence with temporal and inter-organellar coordination of transcriptome in Arabidopsis. *Plant Physiol.* **171**, 452–467.

Wu, J., Hettenhausen, C., Meldau, S. and Baldwin, I.T. (2007) Herbivory rapidly activates MAPK signaling in attacked and unattacked leaf regions but not between leaves of Nicotiana attenuata. *Plant Cell*, **19**, 1096–1122.

Yang, D.H., Hettenhausen, C., Baldwin, I.T. and Wu, J. (2012) Silencing Nicotiana attenuata calcium-dependent protein kinases, CDPK4 and CDPK5, strongly up-regulates wound- and herbivory-induced jasmonic acid accumulations. *Plant Physiol.* **159**, 1591–1607.

Ye, Z., Rodriguez, R., Tran, A., Hoang, H., de los Santos, D., Brown, S. and Vellanoweth, R.L. (2000) The developmental transition to flowering represses ascorbate peroxidase activity and induces enzymatic lipid peroxidation in leaf tissue in Arabidopsis thaliana. *Plant Sci.* **158**, 115–127.

Yoo, S.C., Cho, S.H., Zhang, H. *et al.* (2007) Quantitative trait loci associated with functional stay-green SNU-SG1 in rice. *Mol. Cells*, **24**, 83–94.

Yuree, L., Rubio, M.C., Julien, A. and Niko, G. (2013) A mechanism for localized lignin deposition in the endodermis. *Cell*, **153**, 402–412.

Zhang, K., Halitschke, R., Yin, C., Liu, C.J. and Gan, S.S. (2013) Salicylic acid 3-hydroxylase regulates Arabidopsis leaf longevity by mediating salicylic acid catabolism. *Proc. Natl. Acad. Sci. USA*, **110**, 14807–14812.

Zhang, S., Li, C., Wang, R. *et al.* (2017) The Arabidopsis mitochondrial protease FtSH4 is involved in leaf senescence via regulation of WRKY-dependent salicylic acid accumulation and signaling. *Plant Physiol.* **173**, 2294–2307.

Zhang, Y. and Li, X. (2019) Salicylic acid: biosynthesis, perception, and contributions to plant immunity. *Curr. Opin. Plant Biol.* **50**, 29–36.

Zhou, X., Jiang, Y. and Yu, D. (2011) WRKY22 transcription factor mediates dark-induced leaf senescence in Arabidopsis. *Mol. Cells*, **31**, 303–313.

Zimmermann, P., Heinlein, C., Orendi, G. and Zentgraf, U. (2006) Senescence-specific regulation of catalases in Arabidopsis thaliana (L.) Heynh. *Plant Cell Environ.* **29**, 1049–1060.